

Titan Atmospheric Composition by Hypervelocity Shock-Layer Analysis

H. F. Nelson*

University of Missouri-Rolla, Rolla, Missouri 65401

Chul Park†

NASA Ames Research Center, Moffett Field, California 94035

and

Ellis E. Whiting‡

Eloret Institute, Sunnyvale, California 94087

Planning is currently underway to send a probe into the atmosphere of Titan (a moon of Saturn) as part of the Cassini Mission. This paper presents an investigation of the feasibility of determining the mole fractions of the major species in Titan's atmosphere (N_2 , CH_4 , and argon, if present) using a radiometer to measure the CN(violet) radiation emitted in the probe's shock layer during the high-velocity portion of the entry. Radiative heating rates spectra are calculated at the probe stagnation point for altitudes near peak heating where the shock-layer gases are in chemical and thermal nonequilibrium. The analysis indicates that the sensitivity of the CN(violet) radiation to the atmospheric composition enables the mole fractions of N_2 , CH_4 , and argon to be determined to about ± 0.015 , ± 0.003 , and ± 0.01 , respectively. These values are much less than the current uncertainties. The maximum nonequilibrium radiative heating rate is predicted to be about half of the maximum convective heating rate. (Prior equilibrium calculations had shown that the radiative heating rate was negligible.) Thus, the beryllium heat shield currently planned may be underdesigned, because it has been developed for convective heating only.

Introduction

TITAN is Saturn's largest moon and the only moon in the solar system with a substantial atmosphere. Its surface pressure is about 50% higher than the Earth's. The atmosphere is opaque, with multiple layers of aerosols, ranging from thin smog-like hazes to thick clouds of frozen, or liquid, methane. It is thought that the organic chemistry in Titan's atmosphere may resemble that of the Earth's primitive atmosphere before life began. Consequently, Titan is of high scientific interest.

An atmosphere was first detected on Titan in 1908 by Sola¹ from visual observations of limb darkening. Methane was discovered in Titan's atmosphere in 1944 by Kuiper² from near-infrared spectra. The most current and accurate information of Titan's atmosphere was obtained during Voyager 1 and 2 Saturn flyby missions in 1980 and 1981.³⁻⁵ The atmosphere is now known to be composed mainly of molecular nitrogen, methane, hydrogen, possibly argon, and a number of minor species containing H, C, and O. However, the specific mole fractions of the three major species, N_2 , CH_4 , and possibly argon, are not well defined.

The composition of Titan's atmosphere and its uncertainties are discussed by Hunten et al.⁶ A summary of their data is given in Table 1, taken directly from their report. This table shows the atmospheric composition for pressures below 0.1 mbar (i.e., above an altitude of about 250 km), where the composition is believed to be nearly uniform with altitude. Note the large uncertainties for N_2 (65–98%), CH_4 (2–10%), and argon (0–25%).

The uniformity of the composition over a large altitude range is discussed by Yung et al.,⁷ who performed a photochemical analysis of the atmosphere. They conclude that the composition of the major species is nearly constant from about 50 to 850 km. Based on their analysis, they developed a model for the atmospheric composition containing 2% CH_4 and 0.2% H_2 with the major species being N_2 .

The 1- σ uncertainty range in the mean molecular weight of the atmosphere is specified by Lellouch and Hunten⁸ to be 27.8–29.4 g/mole. If the lower bound is due to a mixture of N_2 and CH_4 only, the composition would be 98.3% N_2 and 1.7% CH_4 . If the upper bound is due to a mixture of N_2 and argon only, it would be 88.3% N_2 and 11.7% argon.

Resolving the uncertainties in Titan's atmospheric composition is a high priority of the Cassini Mission, which will explore Saturn and its system of rings and satellites. A brief description of the Cassini Mission is given in the next section.

Cassini Mission and Titan Probe

The proposed Cassini Mission is an international cooperative project between NASA and the European Space Agency (ESA) to explore Saturn and its moons. One of its major focal points is the investigation of the atmosphere of Titan.⁹⁻¹⁷

The Cassini spacecraft includes a Saturn orbiter (Mariner Mark II spacecraft) and a Titan atmospheric entry probe (Huygens probe). Launch is planned for April 1996. The interplanetary trajectory uses gravity assist at both Earth and Jupiter to reach Saturn in December 2002 after a flight time of 6.8 yr. A schematic diagram of the baseline mission trajectory

Presented as Paper 89-1770 at the AIAA 24th Thermophysics Conference, Buffalo, NY, June 12–14, 1989; received June 23, 1989; revision received Dec. 18, 1989; accepted for publication Dec. 22, 1989. Copyright © 1989 by the American Institute of Aeronautics and Astronautics, Inc. No copyright is asserted in the United States under Title 17, U.S. Code. The U.S. Government has a royalty-free license to exercise all rights under the copyright claimed herein for Governmental purposes. All other rights are reserved by the copyright owner.

*Professor of Aerospace Engineering, Thermal Radiative Transfer Group, Department of Mechanical and Aerospace Engineering. Associate Fellow AIAA.

†Research Scientist. Associate Fellow AIAA.

‡Research Scientist.

Table 1 Atmospheric composition of Titan below 0.1 mbar

Gas	Band	Position, cm ⁻¹	Mole fraction	
			Inferred indirectly	Measured directly
Nitrogen	N ₂	—	—	0.65-0.98
Argon (?)	Ar	—	—	0-0.25
Methane	CH ₄	ν_4	1304	0.02-0.10
Hydrogen	H ₂	S_0	360	2×10^{-3}
		S_1	600	
Carbon monoxide	CO	(3-0)	6350	6×10^{-5}
		$\chi^1\Sigma^+$		-1.5×10^{-4}
Ethane	C ₂ H ₆	ν_9	821	2×10^{-5}
Propane	C ₃ H ₈	ν_{21}	748	4×10^{-6}
Acetylene	C ₂ H ₂	ν_5	729	2×10^{-6}
Ethylene	C ₂ H ₄	ν_7	950	4×10^{-7}
Hydrogen cyanide	HCN	ν_2	712	2×10^{-7}
Methyl acetylene	C ₃ H ₄	ν_9	633	3×10^{-8}
		ν_{10}	328	
Diacyetylene	C ₄ H ₂	ν_8	628	$\sim 10^{-8} - 10^{-7}$
		ν_9	220	
Cyanoacetylene	HC ₃ N	ν_5	663	$\sim 10^{-8} - 10^{-7}$
		ν_6	499	
Cyanogen	C ₂ N ₂	ν_5	233	$\sim 10^{-8} - 10^{-7}$
Carbon dioxide	CO ₂	ν_2	667	1.5×10^{-9}

to Saturn is shown in Fig. 1, which is taken from Ref. 12. The dots along the trajectory represent the approximate distance traveled in 50 days.

The Titan probe will be carried to Saturn by the orbiter. Both the orbiter and probe will be propulsively inserted into an orbit around Saturn. The probe is targeted for Titan and separated from the orbiter during the first orbit. It subsequently enters and descends through Titan's atmosphere as shown schematically in Fig. 2. Deploying the probe from an orbit about Saturn, rather than directly from the interplanetary trajectory, reduces its entry velocity from about 11 km/s to as low as 5.5 km/s.

Atmospheric entry is arbitrarily defined to begin at 1000 km altitude. The high-speed portion of the entry lasts for 2-3 min, during which time the probe descends to about 200 km and its velocity is reduced to about 400 m/s (approximately Mach 1.5). At this point the decelerator section of the heat shield and the beryllium nose cap are released, a parachute is deployed, and the scientific instruments that operate during the final descent and on the surface are activated. The time for data acquisition in the lower atmosphere before the probe hits the surface is about 3 h. Although landing survival is not required in the mission plan, there could be as much as 30 min after impact for acquiring scientific data on the surface before the orbiter moves out of transmission range.

The high-speed portion of the flight is characterized by the formation of a strong bow shock wave and a high-temperature shock layer (4000-6000 K at equilibrium) ahead of the vehicle that will emit optical radiation. This provides the opportunity to determine the mole fractions of the major species in the atmosphere by a shock-layer radiometer experiment.

Radiometer Experiment Contributions to the Titan Probe Mission

The present Cassini Mission plan calls for the atmospheric composition of Titan to be determined below about 170 km by a gas chromatograph/mass spectrometer (GCMS) experiment on the probe.¹⁸ A second mass spectrometer on the orbiter, which will pass through the upper part of the Titan atmosphere (above 800 km) nearly 40 times during its planned lifetime of four years,¹⁸ will determine the composition at very high altitudes. In addition, during each orbiter pass, remote measurements of scattering and emission from the lower atmosphere will be made. In the current mission plan, no instru-

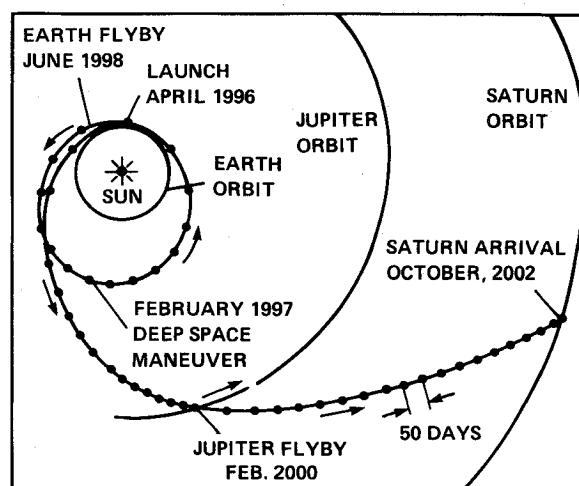


Fig. 1 Schematic diagram of the Cassini baseline mission.

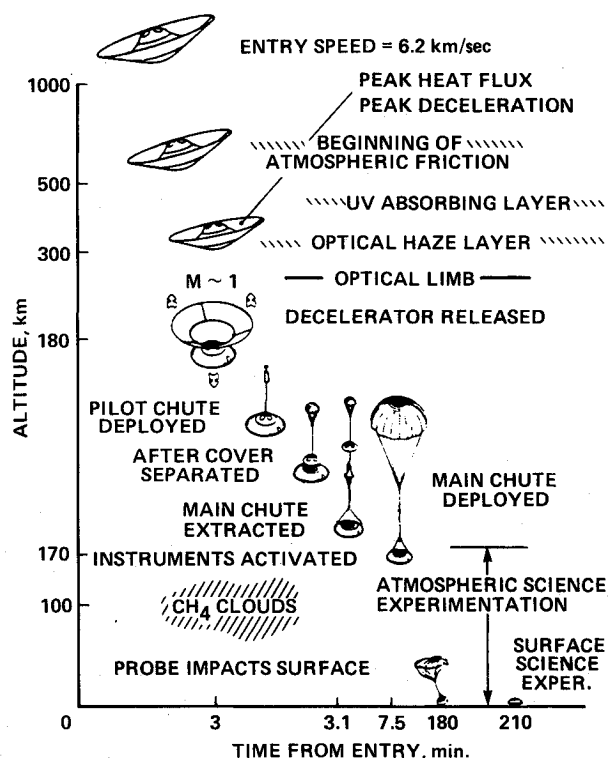


Fig. 2 Schematic diagram of the Titan probe atmospheric entry.

ment is proposed to provide direct composition measurements in the 170- to 800-km-altitude range.

A shock-layer radiometer could provide a direct and independent composition measurement over about half of this range. It is a proven concept for determining the composition of a planetary atmosphere during the high-speed portion of an entry trajectory. The concept was verified during an actual entry flight into the Earth's atmosphere in 1972 in the Planetary Atmosphere Experiment Test (PAET).¹⁹

Results from the PAET radiometer experiment are shown in Figs. 3 and 4, which are taken from Ref. 19. The data points and calculated curves plotted in Fig. 3 for the nitrogen channel, which measured mainly the N₂⁺ (0,0) band, and in Fig. 4 for the CN channel, which measured mainly the CN(violet), $\Delta v = 0$ sequence, illustrate the sensitivity of the spectral band radiation to the atmospheric composition. Both the maximum intensities and the shapes of the radiation pulses are functions of the composition. The figures show (for an assumed air mixture of N₂, O₂, and CO₂, whose N₂/O₂ ratio is 4) that the CO₂ mole fraction must be very close to the known air value of

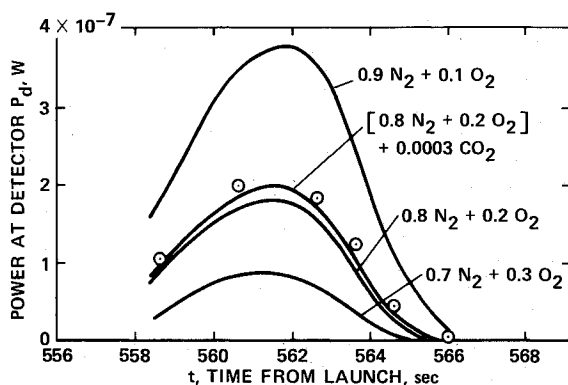
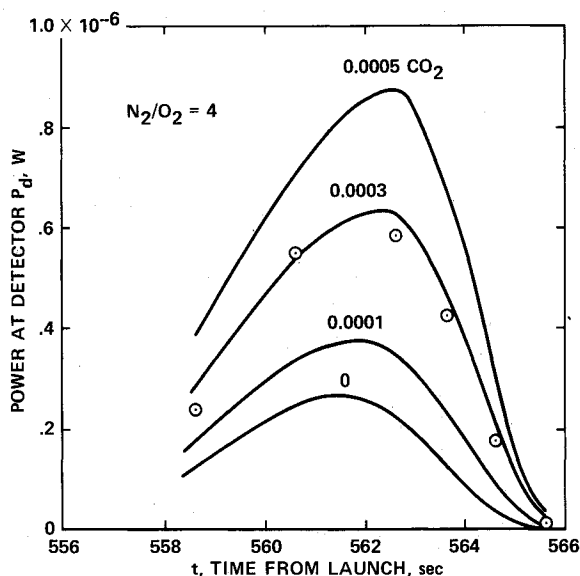
Fig. 3 PAET data and theory for the nitrogen (N_2^+) channel.

Fig. 4 PAET data and theory for the CN(violet) channel.

0.0003 to agree with the data. The accurate determination of the small amount of CO_2 present is due to the high sensitivity of the CN(violet) radiation to a small amount of carbon in a predominantly nitrogen gas mixture at temperatures of 4000–8000 K. These conditions are similar to those expected in the shock layer during the Titan entry.

Titan's atmosphere between about 200 and 400 km appears to be nearly ideal for a radiometer experiment. There are only two or three major atmospheric species. Under the proposed entry conditions, CN will readily form in the shock layer, and it is well known that the CN(violet) bands radiate strongly in an easily accessible portion of the spectrum near 390 nm. The analysis presented later in this paper shows that the intensity of CN(violet) radiation and its variation along the trajectory are sensitive to the relative amounts of N_2 , CH_4 , and argon in the atmosphere. In fact, it appears that only a two-channel radiometer is necessary: one to measure the CN(violet) radiation and one to measure the nearby background. However, it seems desirable to carry a few additional channels for redundancy and perhaps to guard against surprises. Further work is necessary to define an optimum instrument.

Shock-Layer Radiometer Experiment

The proposed Titan shock-layer radiometer experiment is modeled closely after the successful radiometer experiment carried on the PAET¹⁹ vehicle during a high-speed entry into the Earth's atmosphere. The PAET experiment demonstrated that this simple method could accurately determine the composition of an atmosphere composed of a few major species (four in the case of Earth, but only two or three in the case of Titan).

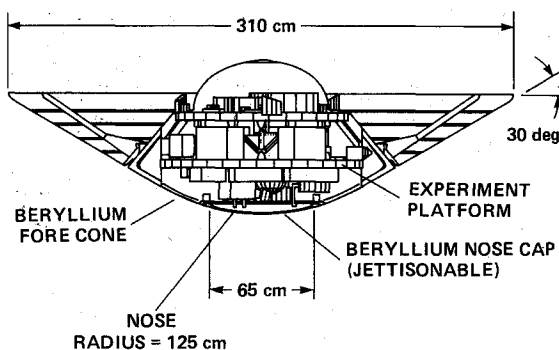


Fig. 5 Titan probe with its decelerator extended.

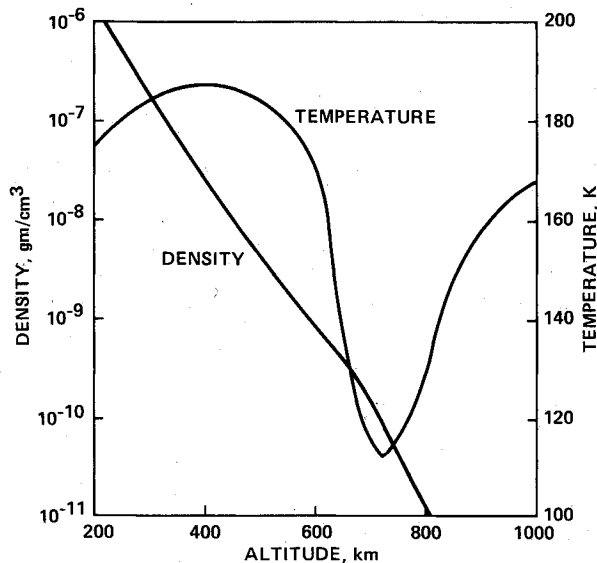


Fig. 6 Titan atmospheric density and temperature as a function of altitude.

The proposed Titan probe configuration is described in the Cassini phase A study¹⁸ and is illustrated in Fig. 5, which is taken from Ref. 18. Details of the scientific instrumentation are given in Refs. 12 and 18. When the decelerator is fully deployed, the probe forebody is a spherical blunted cone with a nose radius of 125 cm. In this configuration the probe mass is expected to be about 192 kg, and its ballistic coefficient is expected to be 20.2 kg/m^2 , which by design is small enough so that deceleration takes place above Titan's cloud layer.

The probe design is quite compact. However, the proposed design has a small space (about 3.5 cm high) on the symmetry axis between the beryllium nose cap and the first permanent structural wall that is not designated for any equipment. This space should provide adequate volume for a window through the heat shield, its necessary support structure, and a small radiometer of 2–10 channels. It might be necessary to include a turning mirror so that the channels could be oriented perpendicular to, rather than parallel to, the probe axis, but this would not cause any difficulty to the experiment.

A radiometer is a simple, rugged instrument. It has no moving parts and can be calibrated prior to entry simply by being pointed at the sun. It can be made very small and light and will fit on the probe, as presently proposed, without disturbing the other instruments in any significant way. It would require a window in the beryllium nose cap near the stagnation point, but the entry conditions are not excessively severe; thus, an acceptable window design should not be difficult.

Atmospheric Entry

The currently accepted engineering model for the density and temperature of Titan's atmosphere was developed by Lellouch and Hunten in 1987.⁸ Their values of the temperature

and nominal density are shown as a function of altitude in the range of 200–1000 km in Fig. 6.

The atmospheric entry trajectory considered in this study is a vertical flight path (entry angle of -90 deg) with a velocity of 6.22 km/s at 1000 km altitude (see Fig. 2). The velocity of the probe and its deceleration as a function of altitude for the nominal atmospheric model are shown in Fig. 7. Table 2 gives specific trajectory data at 6-s intervals over the altitude range of about 400–200 km, where significant optical radiation is emitted in the shock layer.

Shock-Layer Analysis

The present shock-layer analysis is based on continuum flow theory. A simplified treatment of rarefied flow was developed by Adams and Probst²⁰ to show that the free-stream Knudsen number (Kn = molecular mean free path / characteristic length) based on vehicle base diameter is comparable to Kn in the shock layer based on the shock stand-off distance. Continuum theory applies to situations where Kn is less than about 1. Using the atmospheric model and a Titan probe base diameter of 310 cm, which corresponds to a shock stand-off of about 10 cm, continuum theory applies for altitudes below 700 km, where the molecular mean free path in the shock layer is about 1.2 cm and $Kn = 0.12$. Peak shock-layer radiative emission occurs near the peak deceleration point of the entry trajectory. Thus, from Fig. 7, the maximum radiative emission occurs at approximately 250 km, where the use of continuum theory is clearly justified.

Even though the use of continuum theory is justified for the Titan entry shock-layer calculations, it does not necessarily follow that the gas in the shock layer will be in either chemical or thermal equilibrium. Park²¹ recently investigated the conditions for thermal and chemical nonequilibrium in nitrogen shock layers. He presented characteristic times for the radiative emission to reach its peak value and to relax to its equilibrium value as a function of freestream velocity and pressure. Considering the Titan trajectory point at 112 s from Table 2 (5.231 km/s and 8.0 Pa) and using Fig. 8 of Ref. 21 yields the characteristic time to reach peak emission of 13 μ s and to relax to thermodynamic equilibrium of 126 μ s. These times, when multiplied by the freestream velocity, indicate that peak emission occurs about 7 cm behind the shock wave, and thermodynamic equilibrium occurs at about 66 cm. The shock stand-off distance at this point on the Titan entry trajec-

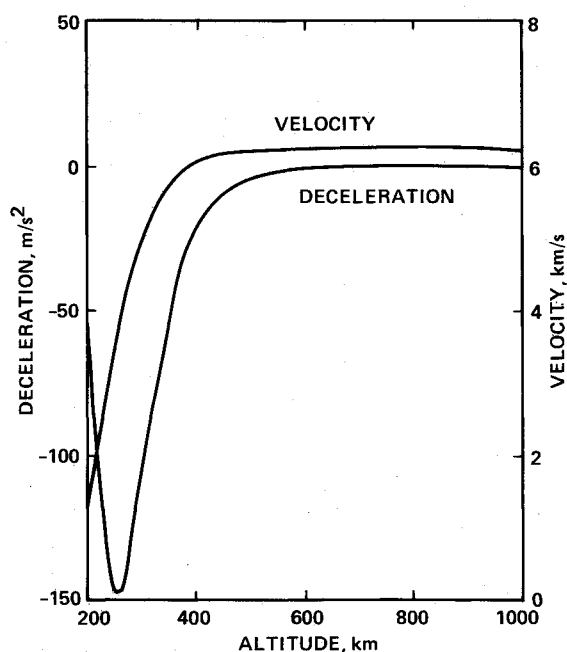


Fig. 7 Titan probe deceleration and velocity as a function of altitude ($v = 6.22$ km/s at 1000 km, entry angle = -90 deg).

tory is only about 10 cm; therefore, thermal and chemical nonequilibrium effects must be accounted for in the shock layer. Thus, shock-layer composition and radiation were calculated using the one-dimensional, nonequilibrium computer code, Stagnation Point Radiation Program (SPRAP), which was developed for shock waves in air.^{22,23} In the current work a modified version of SPRAP that includes carbon, hydrogen, and noble gas species was used. The details of the modification have not been published.

The SPRAP code contains an extensive chemical and thermal nonequilibrium model. It has been shown to give good results when compared to Earth entry and shock-tube experimental data taken under nonequilibrium conditions. The code integrates the time-dependent conservation equations to steady state for one-dimensional flow through a shock wave accounting for viscous transport effects. A two-temperature model (TT_v model) is used in the chemistry portion of the code.^{21,24} One temperature (T) represents the heavy particle translation and rotational temperatures, and a second temperature (T_v) represents the electronic, vibrational, and electron translational temperatures. This model gives good results because of the very rapid energy exchange that occurs between 1) the heavy particle kinetic energy and the molecular rotational energy modes and 2) the free electrons and both the electronic and vibrational energy modes. The reactions and

Table 2 Atmospheric entry conditions nominal atmosphere density profile

$V_0 = 6.220$ km/s, -90 deg Entry						
Time, s	Altitude, km	Velocity, km/s	Density, kg/m ³	P, Pa	T, K	Deceleration, m/s ²
94	413.5	6.122	2.01E-05	1.13	187	17.66
100	377.2	5.973	3.90E-05	2.19	187	33.52
106	342.1	5.699	7.58E-05	4.23	186	60.05
112	309.2	5.231	1.45E-04	8.00	185	97.07
118	279.8	4.535	2.62E-04	14.37	183	132.80
124	255.1	3.678	4.44E-04	24.03	181	147.80
130	235.6	2.825	6.76E-04	36.29	179	132.80

Table 3 Chemical reaction rate constants

Reaction	Reaction energy, kcal/mole	C, cm ³ /mole-s	n	E/R, K
Dissociation reactions ($T_i = \sqrt{TT_v}$)				
$C_2 + M \rightleftharpoons C + C + M$	-141.75	9.68E+22	-2.0	71000
$N_2 + M \rightleftharpoons N + N + M$	-225.06	3.70E+21	-1.6	113200
$CH + M \rightleftharpoons C + H + M$	-80.44	1.13E+19	-1.0	40913
$CN + M \rightleftharpoons C + N + M$	-178.11	1.00E+23	-2.0	90000
$CH_4 + M \rightleftharpoons CH_3 + H + M$	-103.24	2.25E+27	-1.87	52900
$CH_3 + M \rightleftharpoons CH_2 + H + M$	-108.25	2.25E+27	-1.87	54470
$CH_2 + M \rightleftharpoons CH + H + M$	-100.57	2.25E+27	-1.87	50590
$NH + M \rightleftharpoons N + H + M$	-74.18	1.13E+19	-1.0	41820
$H_2 + M \rightleftharpoons H + H + M$	-103.27	1.47E+19	-1.23	51950
Exchange reactions ($T_i = T$)				
$C + N_2 \rightleftharpoons CN + N$	-46.95	1.11E+14	-0.11	23000
$CN + C \rightleftharpoons C_2 + N$	-36.36	3.00E+14	0.00	18120
$C_2 + N_2 \rightleftharpoons CN + CN$	-10.59	7.10E+13	0.00	5330
$H + N_2 \rightleftharpoons NH + N$	-150.88	2.20E+14	0.00	71370
$H_2 + C \rightleftharpoons CH + H$	-22.83	1.80E+14	0.00	11490
$CN^+ + N \rightleftharpoons CN + N^+$	-10.96	9.80E+12	0.00	40700
$C + N \rightleftharpoons CN^+ + e^-$	-146.09	1.00E+15	1.50	164440
$C^+ + N_2 \rightleftharpoons N_2^+ + C$	-99.63	1.11E+14	-0.11	50000
Associative ionization reaction ($T_i = T$)				
$N + N \rightleftharpoons N_2^+ + e^-$	-134.24	1.79E+09	0.77	67500
Ionization reactions ($T_i = T_v$)				
$N + M \rightleftharpoons N^+ + e^- + M$	-335.17	2.50E+34	-3.82	168600
$C + M \rightleftharpoons C^+ + e^- + M$	-259.67	3.90E+33	-3.78	130000
$H + M \rightleftharpoons H^+ + e^- + M$	-313.59	5.90E+37	-4.00	157800
$Ar + M \rightleftharpoons Ar^+ + e^- + M$	-363.25	2.50E+34	-3.82	181700

Note: rate = $CT_i^n \exp [-E/RT_i]$, where $T_i = T, T_v$ or $\sqrt{TT_v}$

reaction rates used for the present calculations are given in Table 3.

Although this work is based on calculations using a one-dimensional shock-layer code and reaction rates that may not be precise, it is believed that the sensitivity shown in the analysis is representative of that which will occur in the actual entry. The actual measured intensity levels may be somewhat different from those calculated; however, the sensitivity to composition will be about the same.

The ability to calculate the full three-dimensional nonequilibrium, viscous flowfield around entry vehicles is under active development at the present time. It is being carried forward, in part, by the Aeroassist Flight Experiment (AFE) program,^{25,26} which is focused to obtain the technology base needed to design advanced entry vehicles. The AFE vehicle is scheduled for launch from the Shuttle in 1994. The experimental radiative data obtained from this program (using radiometers similar to those proposed for the Titan probe) will be used to validate and improve flowfield computer codes and algorithms. Thus, shock-layer computational capabilities will be greatly advanced beyond the current capability by the time of the Titan entry. However, nonequilibrium data analysis does not depend solely on advanced flowfield codes. It can also be performed empirically by a comparison to shock-tube experimental data, as was done for PAET.²⁷ The Titan probe shock-layer radiometer experiment will provide important additional new data on shock-layer structure that will help to further advance the critical technology of atmospheric entry.

Table 4 Atmospheric compositions used in analysis

N_2/CH_4 ratio	Argon mole fraction, %	Mean molecular weight, gm/mole
99/1	0	27.88
98/2	0	27.76
96/4	0	27.52
90/10	0	26.80
99/1	5	28.48
98/2	5	28.37
96/4	5	28.15
90/10	5	27.46
99/1	10	29.09
98/2	10	28.99
96/4	10	28.77
90/10	10	28.12

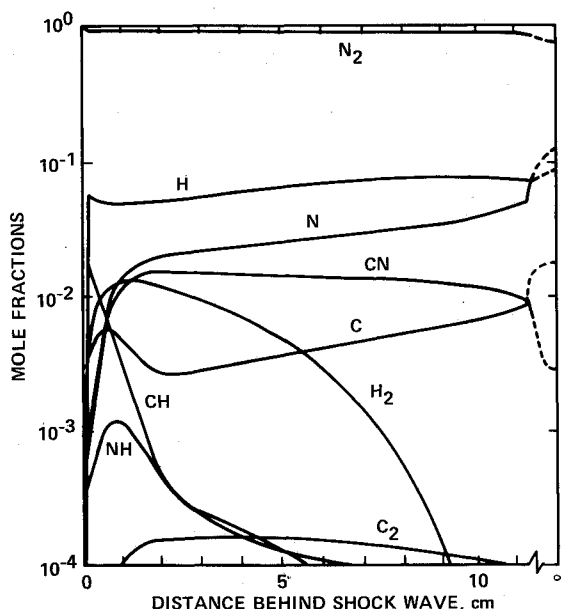


Fig. 8 Species mole fraction as a function of position in the Titan probe shock layer ($t = 118$ s, altitude = 280 km, $N_2/CH_4 = 98/2$, argon = 0%).

Radiation Calculations

Shock-layer calculations were made for the 12 atmospheric compositions given in Table 4 to provide a realistic picture of the sensitivity of a shock-layer radiometer experiment to atmospheric composition. The compositions were selected to provide a reasonable coverage of the uncertainties given in Table 1 and to include a composition close to that of Yung et al.⁷ Mixture ratios for N_2/CH_4 of 99/1, 98/2, 96/4, and 90/10 were chosen. For each of these ratios, calculations were made for argon molar percentages of 0, 5, and 10%. The mean molecular weight for each mixture is also given in Table 4.

Typical results from the calculations are shown in Figs. 8-11. These figures show results for a gas mixture with a N_2/CH_4 ratio of 98/2 and 0% argon, which is very close to Yung's model atmospheric composition.⁷ The species mole fractions are plotted in Fig. 8 as a function of the distance behind the shock wave for the trajectory point at 118 s after the 1000-km starting point (see Table 2). For this case the shock stand-off distance is 11.3 cm. Also shown in this figure are the mole fractions that would result if the shock layer was in ther-

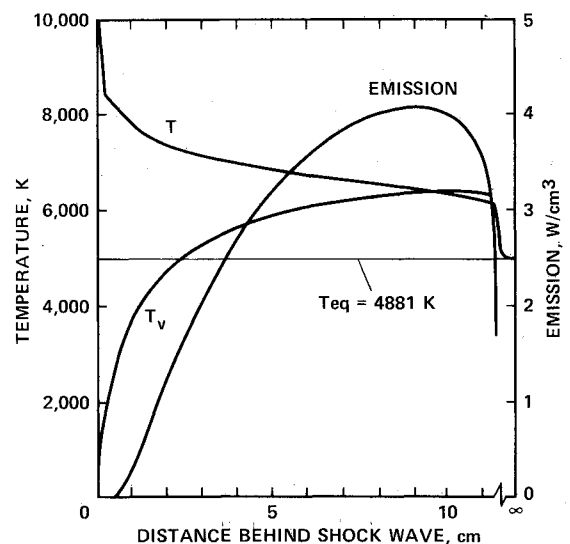


Fig. 9 Temperatures and spontaneous emission from CN(violet) and CN(red) position in the Titan probe shock layer ($t = 118$ s, altitude = 280 km, $N_2/CH_4 = 98/2$, argon = 0%).

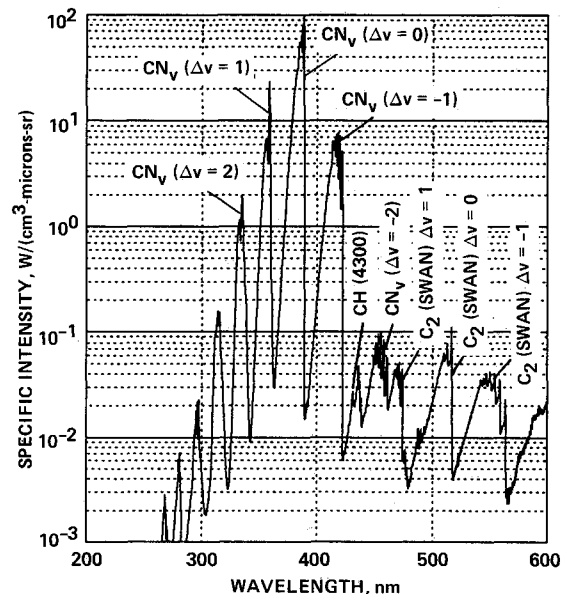


Fig. 10 Spontaneous emission from a nonequilibrium shock layer near its maximum emission point ($t = 118$ s, altitude = 280 km, $N_2/CH_4 = 98/2$, argon = 0%).

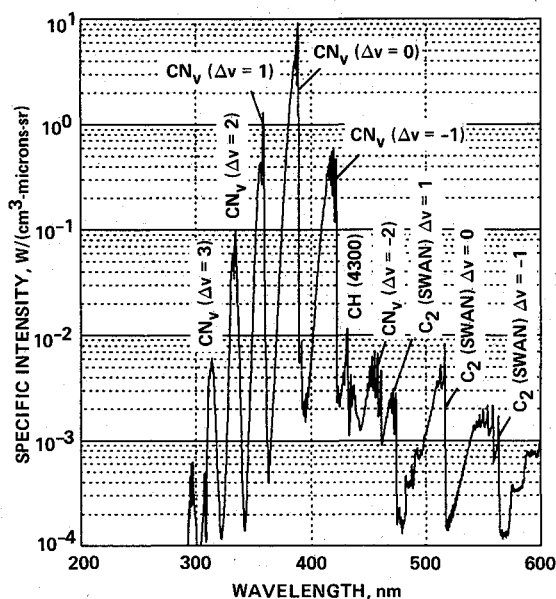


Fig. 11 Spontaneous emission from an equilibrium shock layer for same conditions specified in Fig. 10.

modynamic equilibrium. These values are denoted by the dashed curves that connect with the right vertical axis labeled with the infinity symbol.

Notice that all of the diatomic molecules that form in the shock layer (CN, H₂, CH, NH, and C₂) overshoot their equilibrium values very near the shock wave, but only CN and C₂ maintain these values across most of the shock layer. The mole fraction of CN across most of the shock layer is much higher (about a factor of 5) than its equilibrium value. CN is a very strong radiator, and this result indicates that the nonequilibrium CN radiation is greatly enhanced over its equilibrium value. The CN concentration in the shock layer will be almost linearly proportional to the amount of CH₄ in the atmosphere for small amounts of CH₄.

The CH₄ mole fraction is not shown in Fig. 8 because it dissociates very quickly. This effect is clearly evident, however, in the fast rise in the mole fractions for the species containing carbon and hydrogen atoms just behind the shock wave.

The temperatures T and T_v and the total spontaneous emission (W/cm³) from CN(violet) and CN(red) into 4π steradians and integrated from 200–2000 nm are shown in Fig. 9 for the trajectory point at 118 s. The variables T and T_v are significantly different over most of the shock layer. The heavy particle translational-rotational temperature T decreases as energy is transferred into the vibrational and electronic modes, which causes the vibrational-electronic-electron temperature T_v to increase. Both T and T_v are higher than their equilibrium temperatures of 4881 K across most of the shock layer. Thus, not only will the nonequilibrium CN radiation be enhanced due to the high CN population but also because the electronic temperature is higher than the equilibrium value. This effect is evident in Fig. 9 by the increasing magnitude of the emission across the shock layer as the electronic temperature increases, even though the CN concentration is nearly constant.

The spectral distribution of the spontaneous emission at a point in the shock layer near the maximum value of the emission (approximately 9.5 cm behind the shock wave) is shown in Fig. 10 for wavelengths between 200 and 600 nm. The prominent diatomic band systems in the spectrum are identified. The intensity of the CN(violet) system is about three orders of magnitude greater than any other system in this wavelength region. At longer wavelengths the most intense radiation is from the CN(red) band spectrum. If the gas in the shock layer at this point were in thermodynamic equilibrium, the spectrum would be as shown in Fig. 11. The equilibrium spectrum appears very much like the nonequilibrium spec-

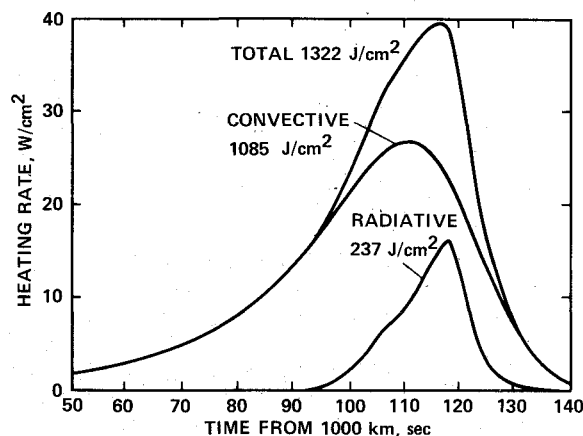


Fig. 12 CN heating rates and total heating during Titan entry ($v = 6.22$ km/s at 1000 km, entry angle = -90 deg, N₂/CH₄ = 98/2, argon = 0%).

trum; however, the nonequilibrium intensities are about an order of magnitude stronger.

Stagnation-Point Heating

The strong nonequilibrium radiation intensity has an important impact on the total heating of the vehicle. The predicted radiative heating rate [from only the CN(violet) and CN(red) systems] and the convective rate are shown in Fig. 12 as a function of time along the entry trajectory. The radiative flux to the surface of the Titan probe was calculated at the points along the trajectory shown in Table 2 for the optically thin, one-dimensional slab approximation and was integrated from 200–2000 nm. The radiative heating rate will be higher when other radiating species are included in the calculation. The convective heating rate was calculated using a correlation equation similar to that given by Tauber²⁸ and Marvin and Deiwert.²⁹

The peak radiative heating rate is 16.2 W/cm² and occurs at 118 s, corresponding to an altitude of 280 km. CN(red) contributes 59% of the maximum rate, whereas CN(violet) contributes 41%. The integrated radiative heating along the trajectory is 237 J/cm². This compares to a total convective value of 1085 J/cm². Thus, radiative heating accounts for roughly 18% of the total heating.

The proposed Titan probe will have a beryllium heat shield that was designed considering only the convective heating load. (The design radiative heating load was calculated assuming thermodynamic equilibrium in the shock layer, which indicated that the radiative heating was negligible.) The nonequilibrium radiative peak heating rate shown in Fig. 12 is roughly one-half of the convective peak heating rate. Thus, the probe heat shield may be underdesigned.

Atmospheric Composition Evaluation

The sensitivity of the CN radiation to the atmospheric composition is shown in Figs. 13–15. The radiative flux (intensity) at the surface due to CN(violet) in the wavelength interval from 380–390 nm is shown in Fig. 13 as a function of the time from the 1000 km altitude for atmospheres with N₂/CH₄ ratios of 99/1, 98/2, 96/4, and 90/10 and no argon. Plots similar to Fig. 13 were also made for atmospheres containing 5 and 10% argon but are not presented here. The main effect of adding argon is to increase the intensity a small amount as the argon content is increased from 0 to 10%.

Time from 1000 km, rather than altitude, is used in the present analysis to investigate the sensitivity of the shock-layer experiment to atmospheric composition. This is appropriate because velocity and all of the properties of the atmosphere at a given altitude, except for composition, are assumed constant. In other words, it is assumed that small changes in at-

mospheric composition do not change the time it takes for the probe to descend to a specific altitude. The density and velocity along the flight path are the controlling parameters, and, during an actual entry, time would be measured from an appropriate reference along the trajectory such as the peak deceleration.

Peak intensity and shape of the radiative pulse (see Fig. 13) are functions of the gas mixture. In the following analysis these two parameters will be used to show how the atmospheric composition can be determined.

Notice in Fig. 13 that the peak intensity increases as CH_4 increases from 1 to 2% and then drops as CH_4 is increased further to 4 and then to 10%. The increase in signal for low amounts of CH_4 is due to the increase in the CN concentration in the shock layer as CH_4 increases. However, CH_4 has a large dissociation energy. It takes 392 kcal to dissociate 1 mole of CH_4 into its atomic fragments.³⁰ This effect tends to lower the temperature in the shock layer as CH_4 dissociates. At the higher concentrations of CH_4 , this effect more than offsets the increase in the CN concentration.

The shapes of the curves in Fig. 13 are visibly different. Generally, the curves become broader and the peak occurs earlier in the entry with increasing CH_4 in the atmosphere. The

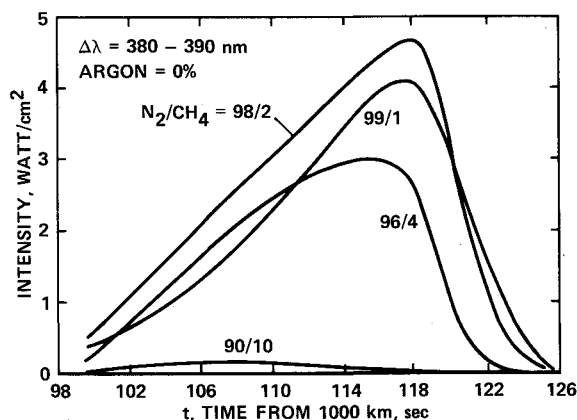


Fig. 13 Radiant flux at stagnation point of Titan probe from CN(violet); $\Delta\nu = 0$ sequence.

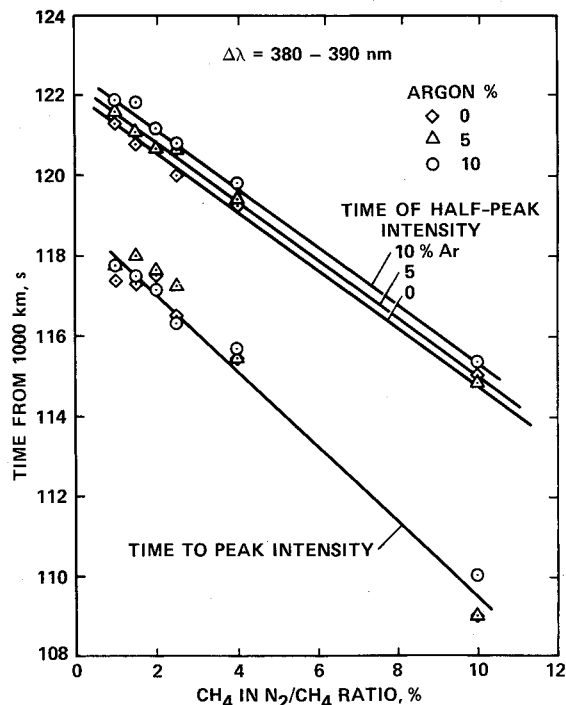


Fig. 14 Radiant pulse shape parameters from CN(violet); $\Delta\nu = 0$ sequence for the Titan probe.

measures of the curve shape used in the present analysis are the time at which the peak intensity occurs and the time at which the intensity falls to half of the peak value (half-peak intensity point). These times are essentially linear with the percent of CH_4 , as shown in Fig. 14, where they are plotted against the percent of CH_4 in the N_2/CH_4 .

The points plotted for the time to peak intensity curve of Fig. 14 show a fair amount of scatter because the precise time at which the peak occurs is difficult to select from the limited number of trajectory points (shown in Table 2) used to define the entry. However, even with this scatter, these points indicate that there is little, if any, effect of argon concentration on the time to peak intensity. Consequently, if the time to peak intensity can be measured to within 0.05 s, which should not be difficult, the mole fraction of CH_4 can be determined within about 0.002–0.003, independent of the peak intensity value. Thus, absolute calibration is not necessary to determine the mole fraction of CH_4 to good accuracy.

The points plotted for the time to half-peak intensity in Fig. 14 show much less scatter and indicate a measurable effect of the argon concentration. Unfortunately, the effect of argon on the time to half-peak intensity is probably not adequate to give a good determination of the argon concentration by itself. Thus, absolute calibration of the radiometer is probably necessary to determine the argon concentration.

The different slopes of the time to peak and time to half-peak curves indicate that the difference in time between the peak intensity value and the half-peak intensity value is likely to be a good measure of the atmospheric composition. Figure 15 shows the sensitivity of the peak in the CN(violet) radiation pulse to the atmospheric composition as a function of the difference in time between peak and half-peak intensity. The solid curves are for 0, 5, and 10% argon, and the dashed curves are for N_2/CH_4 mixture ratios. The possible accuracy of the atmospheric composition determination is also shown in Fig. 15 by the uncertainty indicated in the symbol plotted at 4.0 s and 4.0 W/cm². The uncertainty in measuring the peak intensity is estimated to be 5%, which seems reasonable based on the PAET results. The uncertainty of measuring the time is estimated to be 0.05 s. Based on these uncertainties, Fig. 15 indicates that over most of the range of mixtures shown the mole fraction of CH_4 should be determined to about 0.003, argon to about 0.01, and N_2 , then, to about 0.015. Generally, these are exceptionally good uncertainties. There are some potentially important gas mixtures (near 1–3% CH_4) where the uncertainties will be greater because the solution, as shown in Fig. 15, is multivalued. However, even here the uncertainty of about 0.01 in the mole fraction of CH_4 in the atmosphere would be far better than the range of 0.02–0.10 that currently exists. Fortunately, the redundancy in the CH_4 mole fraction can be resolved by using the time to peak intensity curve (Fig.

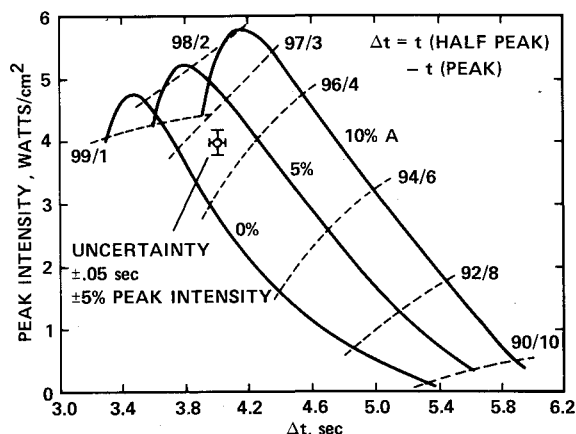


Fig. 15 Peak radiant flux at the stagnation point of the Titan probe from CN(violet); $\Delta\nu = 0$ sequence as a function of atmospheric composition.

14) as mentioned earlier, but some redundancy in the argon mole fraction would remain.

Greater precision in the analysis might be possible by measuring the radiation emitted by other species in the shock layer in addition to CN(violet). For example, the C₂(Swan) sequence near 520 nm shown in Fig. 10 is a possible candidate. This figure shows that, although the intensity of the C₂(Swan) system is much less than that of the CN(violet) system, it is still clearly evident in the spectrum. The CH band at 430 nm is also a possible candidate that includes carbon. However, its radiation is weaker and located, spectrally, closer to the strong CN(violet) system, which would increase the uncertainty of its intensity measurement.

Another method of reducing the uncertainty in the species concentrations would be to combine the radiometric data with the value for the mean molecular weight. The mean molecular weight should be determined accurately below an altitude of 170 km by the density, pressure, and temperature measurements made during the probe's slow descent. The value of the mean molecular weight is believed to be nearly constant from about 50–850 km altitude; thus, the value determined from 50–170 km can be used for the region covered by the shock-layer radiometer experiment: 200–400 km.

Summary and Conclusions

The Titan probe, which is part of the Cassini Mission to Saturn, offers an excellent opportunity to determine the mole fractions of the major species (N₂, CH₄, and argon, if present) in the atmosphere by a shock-layer radiometer experiment during the high-velocity portion of the entry between about 200 and 400 km altitude. The concept for accurately determining atmospheric composition using shock-layer radiometer measurements was demonstrated in 1972 by the PAET Earth atmosphere probe. Titan's atmosphere is an ideal candidate for a shock-layer radiometer experiment because there are only two or three major species in the atmosphere; there is a very strong radiator in the shock layer; and the atmospheric composition is nearly constant over the altitude range where the measurements would be taken.

The present analysis shows that the CN(violet) radiation between 380 and 390 nm is sensitive to the N₂, CH₄, and argon concentrations in the freestream and is a good discriminator of the atmospheric composition. Although this work is based on calculations made using a modified one-dimensional shock-layer code (SPRAP) and on reaction rates that may not be precise, it is believed that the sensitivity shown in the analysis is representative of that which will occur in the actual entry. The actual intensity levels may be somewhat different, but the sensitivity to composition will be about the same.

By using calculated intensities from only the CN(violet) bands, the analysis shows that the mole fractions of the gases in the atmosphere can be determined to about 0.015 for N₂, 0.003 for CH₄, and 0.01 for argon, over a wide range of species concentrations. A background measurement will also be necessary in an actual experiment.

The optimum number of radiometer channels is currently being studied. However, important basic composition data can be obtained with as few as two channels. The radiometer requires minimal space. It could fit just behind the beryllium nose cap and could observe the shock layer through a window near the stagnation point.

The shock-layer radiometer experiment provides a direct measurement of atmospheric composition at altitudes above those accessible to the GCMS, which functions below 170 km. It also provides a backup in case the GCMS experiment should fail. In general, radiometers are reliable, rugged, and relatively inexpensive.

A byproduct of the present study was the finding that the maximum nonequilibrium radiative heating rates are much larger than those for the equilibrium case, and roughly half of the maximum convective heating rates. Previous equilibrium calculations had indicated that radiative heating of the Titan

probe is negligible. As a result, the probe heat shield may be somewhat underdesigned.

Acknowledgments

This work was supported by Intergovernmental Personnel Act Assignment Agreement RT-0076/T-7932 between the University of Missouri-Rolla and NASA Ames Research Center. The authors thank Alvin Seiff of San Jose State University Foundation for his review of the text, advice, and comments and Roger A. Craig and William C. Davy of the NASA Ames Research Center for their support of this work.

References

- ¹Sola, J. C., "Observations des Satellites Principaux de Jupiter et de Titan," *Astronomische Nachrichten*, Vol. 179, 1908, pp. 289.
- ²Kuiper, G. P., "Titan: A Satellite with an Atmosphere," *Astrophysics Journal*, Vol. 100, Nov. 1944, pp. 378–383.
- ³*Science*, Vol. 212, April 10, 1981, entire issue.
- ⁴*Science*, Vol. 215, January 29, 1982, entire issue.
- ⁵*Nature*, Vol. 292, August 20–26, 1981, entire issue.
- ⁶Hunten, D. M., Tomasko, M. G., Flasar, F. M., Samuelson, R. E., Strobel, D. F., and Stevenson, D. J., "Titan," *Saturn*, edited by T. Gehrels and M. S. Matthews, University of Arizona Press, Tucson, AZ, 1984, pp. 671–759.
- ⁷Yung, Y. L., Allen, M., and Pinto, J. P., "Photochemistry of the Atmosphere of Titan: Comparison Between Model and Observations," *Astrophysical Journal Supplement Series*, Vol. 55, July 1984, pp. 465–506.
- ⁸Lellouch, E., and Hunten, D. E., "Titan Atmospheric Engineering Model," European Space Agency Rept. ESLAB 87/199, Oct. 1987.
- ⁹Gautier, D., and Ip, W. H., "Project Cassini: A Saturn Orbiter/Titan Probe Mission Proposal," *Origins of Life*, Vol. 14, 1984, pp. 801–807.
- ¹⁰Raulin, F., Gautier, D., and Ip, W. H., "Exobiology and the Solar System: The Cassini Mission to Titan," *Origins of Life*, Vol. 14, 1984, pp. 817–824.
- ¹¹Scoon, G. E. N., "Cassini—A Concept for a Titan Probe," European Space Agency Bulletin, No. 41, Feb. 1985, pp. 12–20.
- ¹²Scoon, G. E. N., and Flury, W., "Cassini Mission—The Titan Probe," International Aeronautical Federation Paper IAF-87-445, Oct. 1987.
- ¹³Croswell, K., "Titan: Slumbering Giant," *Space World*, Jan. 1988, pp. 20–22.
- ¹⁴Swenson, B. L., Mascy, A. C., Murphy, G. P., and Cuzzi, J. N., "Outer Planet Probe/Flyby Missions," AIAA Paper 83-0522, Jan. 1983.
- ¹⁵Swenson, B. L., Mascy, A. C., and Edsinger, L. E., "A New System Concept for a Titan Atmospheric Probe," AIAA Paper 84-0456, Jan. 1984.
- ¹⁶Swenson, B. L., "Titan Atmospheric Probe," *Journal of the British Interplanetary Society*, Vol. 37, 1984, pp. 366–369.
- ¹⁷Sergeyevsky, A. B., Courage, S. J., and Stetson, D. S., "Cassini—A Mission to the Saturnian System," American Astronautical Society, AAS Paper 87-423, Aug. 1986.
- ¹⁸Gautier, D., Ip, W., and Owen, T., "Cassini, Saturn Orbiter and Titan Probe: Report on the Phase A Study," European Space Agency Rept. SCI(88)5, Oct. 1988.
- ¹⁹Whiting, E. E., Arnold, J. O., Page, W. A., and Reynolds, R. M., "Composition of Earth's Atmosphere by Shock-Layer Radiometry During PAET Entry Probe Experiment," *Journal of Quantitative Spectroscopy and Radiative Transfer*, Vol. 13, Sept. 1973, pp. 837–859.
- ²⁰Adams, M. C., and Probst, R. F., "On the Validity of Continuum Theory for Satellite and Hypersonic Flight Problems at High Altitudes," *Jet Propulsion*, Vol. 28, Feb. 1958, pp. 86–89.
- ²¹Park, C., "Assessment of a Two-Temperature Kinetic Model for Dissociating and Weakly Ionizing Nitrogen," *Journal of Thermophysics and Heat Transfer*, Vol. 2, No. 1, Jan. 1988, pp. 8–16.
- ²²Park, C., "Calculation of Nonequilibrium Radiation in the Flight Regimes of Aeroassisted Orbital Transfer Vehicles," *Progress in Astronautics and Aeronautics: Thermal Design of Aeroassisted Orbital Transfer Vehicles*, Vol. 96, edited by H. F. Nelson, AIAA, New York, 1985, pp. 395–418.
- ²³Park, C., "Problems of Rate Chemistry in Flight Regimes of Aeroassisted Orbital Transfer Vehicles," *Progress in Astronautics and Aeronautics: Thermal Design of Aeroassisted Orbital Transfer*

Vehicles, Vol. 96, edited by H. F. Nelson, AIAA, New York, 1985, pp. 515-537.

²⁴Park, C., "Assessment of Two-Temperature Kinetic Model for Air," *Journal of Thermophysics and Heat Transfer*, Vol. 3, No. 3, July 1989, pp. 233-244.

²⁵Davy, W. C., Park, C., Arnold, J. O., and Balakrishnan, A., "Radiometer Experiment for the Aeroassist Flight Experiment," AIAA Paper 85-0967, June 1985.

²⁶Jones, J. J., "The Rationale For an Aeroassist Flight Experiment," AIAA Paper 87-1508, June 1987.

²⁷Arnold, J. O., and Whiting, E. E., "Nonequilibrium Effects on Shock-Layer Radiometry During Earth Entry," *Journal of Quantitative Spectroscopy and Radiative Transfer*, Vol. 13, Sept. 1973, pp. 861-870.

²⁸Tauber, M. E., "A Review of High-Speed, Convective Heat Transfer Computation Methods," NASA TP-2914, July 1989.

²⁹Marvin, J. G., and Deiwert, G. S., "Convective Heat Transfer in Planetary Gases," NASA TR-224, July 1965.

³⁰McQuarrie, D. A., *Statistical Thermodynamics*, Harper & Row, New York, 1973, Chap. 8.

Attention Journal Authors: Send Us Your Manuscript Disk

AIAA now has equipment that can convert **virtually any disk** (3½-, 5¼-, or 8-inch) **directly to type**, thus avoiding rekeyboarding and subsequent introduction of errors.

The following are examples of easily converted software programs:

- PC or Macintosh T^EX and L^AT^EX
- PC or Macintosh Microsoft Word
- PC Wordstar Professional

You can help us in the following way. If your manuscript was prepared with a word-processing program, please *retain the disk* until the review process has been completed and final revisions have been incorporated in your paper. Then send the Associate Editor *all* of the following:

- Your final version of double-spaced hard copy.
- Original artwork.
- A *copy* of the revised disk (with software identified).

Retain the original disk.

If your revised paper is accepted for publication, the Associate Editor will send the entire package just described to the AIAA Editorial Department for copy editing and typesetting.

Please note that your paper may be typeset in the traditional manner if problems arise during the conversion. A problem may be caused, for instance, by using a "program within a program" (e.g., special mathematical enhancements to word-processing programs). That potential problem may be avoided if you specifically identify the enhancement and the word-processing program.

In any case you will, as always, receive galley proofs before publication. They will reflect all copy and style changes made by the Editorial Department.

We will send you an AIAA tie or scarf (your choice) as a "thank you" for cooperating in our disk conversion program. Just send us a note when you return your galley proofs to let us know which you prefer.

If you have any questions or need further information on disk conversion, please telephone Richard Gaskin, AIAA Production Manager, at (202) 646-7496.

